Sodium channel activation mechanisms

Insights from deuterium oxide substitution

Daniel A. Alicata,* Martin D. Rayner,* and John G. Starkus

Békésy Laboratory of Neurobiology, Pacific Biomedical Research Center, and the *Department of Physiology, John A. Burns School of Medicine, University of Hawaii, Honolulu, Hawaii 96822

ABSTRACT Schauf and Bullock (1979. *Biophys. J.* 27:193–208; 1982. *Biophys. J.* 37:441–452), using *Myxicola* giant axons, demonstrated that solvent substitution with deuterium oxide (D_2O) significantly affects both sodium channel activation and inactivation kinetics without corresponding changes in gating current or tail current rates. They concluded that (*a*) no significant component of gating current derives from the final channel opening step, and (*b*) channels must deactivate (during tail currents) by a different pathway from that used in channel opening. By contrast, Oxford (1981. *J. Gen. Physiol.* 77:1–22) found in squid axons that when a depolarizing pulse is interrupted by a brief (~100 μs) return to holding potential, subsequent reactivation (secondary activation) is very rapid and shows almost monoexponential kinetics. Increasing the interpulse interval resulted in secondary activation rate returning towards control, sigmoid (primary activation) kinetics. He concluded that channels open and close (deactivate) via the same pathway.

We have repeated both sets of observations in crayfish axons, confirming the results obtained in both previous studies, despite the apparently contradictory conclusions reached by these authors. On the other hand, we find that secondary activation after a brief interpulse interval (50 μs) is insensitive to D_2O, although reactivation after longer interpulse intervals (~400 μs) returns towards a D_2O sensitivity similar to that of primary activation. We conclude that D_2O-sensitive primary activation and D_2O-insensitive tail current deactivation involve separate pathways. However, D_2O-insensitive secondary activation involves reversal of the D_2O-insensitive deactivation step. These conclusions are consistent with "parallel gate" models, provided that one gating particle has a substantially reduced effective valence.

INTRODUCTION

The exact relationship between "voltage-sensitive" gating current (I_g), and the molecular events constituting the "opening" or "gating" of the sodium channel remains unclear. Schauf and Bullock (1979, 1980, 1982) and Schauf and Chuman (1986) have reported that solvent substitution of 98% deuterium oxide (D_2O) in *Myxicola* selectively slows macroscopic sodium current kinetics without corresponding action on gating current. No significant component of ON gating current had a time course which followed the altered kinetics of the final channel opening step. Schauf and Bullock (1979) conclude that physiologically detectable gating current must be generated exclusively within nonconducting, preopen transitions of the channel rather than by the movement of the channel "gates" themselves. Furthermore the channel activation gates must be exposed to a hydrophilic phase and hence affected by D_2O, whereas the principle gating current generator appears protected from the effects of solvent substitution. On the other hand, Schauf and Bullock (1982) also observe that closure (deactivation) of conducting sodium channels is insensitive to the effects of D_2O. The rate constants of the fast and slow components of sodium tail current remain unaltered during solvent substitution. The authors suggest that conducting sodium channels may deactivate by a route dissimilar from that taken during initial activation of sodium channels. Schauf (1983) also showed that prepulse-induced ("Cole-Moore-type") shifts in sodium channel activation are not affected by solvent substitution with D_2O.

Structural models describing sodium channel gating have been proposed by Noda et al. (1984), Guy and Seetharamulu (1986), and Catterall (1986). These models suggest that voltage-dependent channel gating results directly from rotation of the highly charged and highly conserved S4 α helix in response to membrane depolarization, such that a significant component of gating charge would move in the final channel opening step. The assumptions of these structural models appear in conflict with the experimental data presented by Schauf and Bullock (1979).

Oxford (1981) demonstrated that when a maintained depolarizing pulse was interrupted by a brief return to

Address correspondence to Daniel A. Alicata, University of Hawaii, Pacific Biomedical Research Center, Békésy Laboratory of Neurobiology, 1993 East West Road, Honolulu, HI 96822. Electronic mail addresses: Internet: alicata @ uhccux. uhec, hawaii, edu. Bitnet: Alicata @ uhccnx.

0006-3495/90/04/745/14 $2.00

holding potential, subsequent reactivation (secondary activation) of the sodium channel proceeded rapidly with almost monoexponential kinetics. During the brief interpulse interval, channels were apparently captured in a nonconducting transition state adjacent to the open state. He concluded that channel deactivation occurs via by reversal of the multistate primary activation path. This evaluation of channel behavior also seems in conflict with a major conclusion reached by Schauf and Bullock (1979, 1982) from their D_2O studies, namely that activation and deactivation occur by separate paths.

We report here the effects of D_2O substitution on sodium channel gating current, ionic current, and tail current in the crayfish. Our results provide detailed confirmation for both Schauf and Bullock's findings in *Myxicola* and Oxford's observations on secondary activation. However, we show that secondary activation, after brief interpulse intervals, is D_2O-insensitive. We present a revised model for sodium channel activation and deactivation which resolves the apparent conflicts noted above. Preliminary results of this work have been presented (Alicata et al., 1989).

METHODS

Medial giant axons from the crayfish, *Procambarus clarkii*, with diameters between 200 and 300 μm, were continuously perfused both internally and externally and voltage clamped with conventional axial wire techniques adapted to crayfish axons by Shrager (1974) and further described by Starkus and Shrager (1978), Rayner and Starkus (1989), and Alicata et al. (1989). Series resistance compensation was set at the value of 10 $\Omega.cm^2$ which removes the dependence of I_{Na} kinetics on changes in current magnitude. Peak I_{Na} was maintained at less than ~1.5 mA/cm^2. Corrections were made for an electrode junction potential of 8–10 mV, and the electrode drift in potential during the course of the experiments reported here did not exceed 1–2 mV. The procedures used for data acquisition, data analysis, and for the subtraction of linear capacity and leakage currents using the -SHP P/n control pulse protocol have been presented in detail by Rayner and Starkus (1989) and Alicata et al. (1989).

Schauf and Bullock (1979) reported from *Myxicola* that D_2O (at 5°C) alters sodium channel kinetics by dramatically slowing the activation and inactivation components of I_{Na}. However, at higher temperatures of 16–18°C sodium channels behaved similarly in H_2O and D_2O thus eliminating kinetic sensitivity of the channel to D_2O action. Our objective was to confirm in crayfish axons the slowing action of D_2O on channel kinetics observed in *Myxicola*. Therefore, we maintained the temperature at 9.5 ± 0.5°C for all the experiments in this study.

Schauf and Bullock (1979, 1980, 1982) and Schauf (1983) exposed both internal and external membrane surfaces to D_2O. In our study D_2O was perfused either internally or externally. We find that D_2O action on sodium channel kinetics is independent of route of application (see Results). When D_2O is perfused internally, the membrane remains stable through 2–3 h of recording. However, when D_2O is placed only on the outside of the axon, crayfish axons remain stable for no more than 15–20 min before a marked increase in the linear leak current is observed, and the membrane becomes increasingly intolerant of capacity current subtraction protocols (P/n) at hyperpolarized potentials. In these experiments D_2O was substituted for H_2O and chilled to ~8–9°C. The volume of the experimental chamber was then exchanged three times and continuously perfused with this prepared solution. Bath temperature equilibrated to 9.5°C within 1 min. The following criteria were therefore established for monitoring membrane integrity: (*a*) the holding current should not exceed that required to maintain membrane voltage within ±0.2 mV of the desired holding potential; (*b*) the peak magnitude of the fast component of linear capacity current could not fluctuate more than ±10% of control conditions; (*c*) the zero time intercepts of the two slower kinetic components of the capacity current should not increase from control levels, and (*d*) leakage current (observed during hyperpolarizing steps) must remain parallel to the baseline and not exceed by >10–20 $\mu A/cm^2$ the measured leakage current in control conditions. We separately recorded the P/n control capacity currents throughout the experiment to check for changes in clamp speed and linear leak (see Alicata et al., 1989). Experiments were terminated when any of the above monitors exceeded criterion levels.

Solutions

The external solution used in this study contained 2.6 mM Mg^{++}, 13.5 mM Ca^{++}, 210 mM tetramethylammonium (TMA), 243 mM Cl^-, and 2.3 mM Hepes, adjusted to pH 7.55. The control internal solution contained 230 mM Cs^+, 60 mM F^-, 170 mM Glu^-, and 1 mM Hepes, adjusted to pH 7.35. Tetrodotoxin (TTX), obtained from Calbiochem-Behring Corp. (La Jolla, CA), was included at 200 nM for all gating current recordings. For experiments involving ionic currents, sodium was partially substituted for TMA in the external solution and Cs^+ was substituted in the internal solution. The sodium ion concentrations are noted in the figure legend as ($[Na]_{in}//[Na]_{out}$). In heavy water experiments, internal and/or external solutions were prepared with 99.8% deuterium oxide (Sigma Chemical Co., St. Louis, MO). In experiments involving chloramine-T (Sigma Chemical Co.) we prepared the internal solution closely following the procedures described by Huang et al. (1987). Optimal results were achieved using freshly prepared 10 mM chloramine-T at pH 6.30. Because chloramine-T also blocks the sodium channel (Wang et al., 1985; Huang et al., 1987), the internal chloramine-T perfusate was washed out as soon as reduction in peak current magnitude of I_{Na} was noticed.

RESULTS

The initial purpose of this project was to confirm in crayfish axons the observations reviewed by Schauf and Chuman (1986) concerning the effects of D_2O on sodium channel kinetics in *Myxicola*. We find that solvent substitution with D_2O significantly slows sodium channel activation and inactivation kinetics (Fig. 1 *A*, and Fig. 3, *A–C*) in crayfish without corresponding changes in tail current kinetics (Fig. 1 *A*) or the ON and OFF gating current (Fig. 1 *B*). Ionic current (Fig. 1 *A*) was recorded before (trace *a*), during (trace *b*), and after (trace *c*) washout of internally perfused D_2O. It is clearly visible that activation and inactivation kinetics of I_{Na} are slowed by D_2O (trace *b*) in comparison to the records in H_2O (traces *a* and *c*). The tail currents (Fig. 1 *A*), however, are indistinguishable and appear insensitive to D_2O action. In Fig. 1 *B* we show records of I_gON and I_gOFF taken in H_2O (trace *a*) and in D_2O (trace *b*). No kinetic

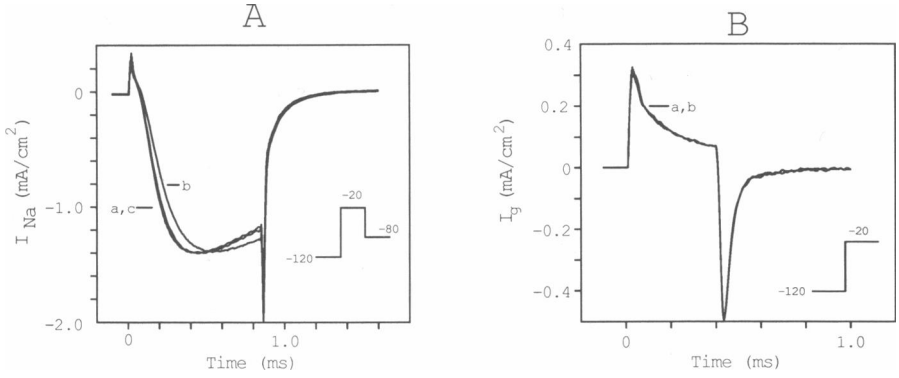

FIGURE 1 D_2O slows I_{Na} activation without affecting tail current or gating current. (*A*) Activation (at −20 mV) and deactivation (at −80 mV) of sodium currents before (trace *a*), during (trace *b*), and after (trace *c*) internal D_2O perfusion. Traces in D_2O are scaled to match peak I_{Na} in H_2O for comparison of kinetic changes. Holding potential was −120 mV. Data from axon 890726, (D_2O, 20 Na//H_2O, 50 Na). (*B*) ON and OFF gating current at −20 mV before (trace *a*) and during (trace *b*) external D_2O perfusion. Holding potential, −120 mV. Data from axon 881115, (0 Na//D_2O, TTX, 0 Na).

effects of D_2O on I_g are apparent at this level of resolution. Thus this figure provides a preliminary confirmation of the major findings reported from *Myxicola* axons. D_2O significantly slows I_{Na} activation and inactivation kinetics without corresponding affect on gating current and ionic tail current (Schauf and Bullock, 1979, 1982; Schauf, 1983; Schauf and Chuman, 1986).

More careful examination of the effects of D_2O on I_gON kinetics (Fig. 2) shows small changes in the initial peak I_gON during exposure to D_2O as noted by Schauf and Bullock (1979). Small changes in peak I_g were also detected in our data, although this is not clearly visible in Fig. 2, *A* or *B*, due to the compressed time base. However, Alicata et al. (1989) have demonstrated that changes in series resistance (R_s) alter clamp rise time, thus affecting both capacity current waveform and the fast component of gating current. We therefore looked for changes in R_s during the course of the experiment by using the waveform of the separately recorded P/n control capacity currents as an indicator of changes in clamp rise time. D_2O induced a small reduction in peak capacity current (<10%) which corresponds to an increase in R_s and a reduction in clamp speed. In every instance in which reduction of peak I_g was noted, we also noted a corresponding reduction in peak capacity current. We conclude that changes in peak I_g result from indirect effects of D_2O on R_s rather than from direct solvent action on the gating currents.

Fig. 2 shows that no D_2O-induced changes are readily apparent in the slower components of gating current. However, integrations of these gating current records suggest small (but consistent) rate changes in charge movement between the records in H_2O (traces *a*) and in D_2O (traces *b*). Gating current was integrated over a 2-ms time course, and there was essentially no change in total charge movement between H_2O and D_2O conditions (see figure legend). The gating currents in Fig. 2, *A* and *B*, were recorded at 0 mV where total charge movement is close to Q_{max} (see Fig. 6 of Rayner and Starkus, 1989) and I_g kinetics are still relatively slow. These conditions maximize the opportunity for recording small kinetic changes in gating currents. Our results confirm the lack of major effect on I_g kinetics noted in *Myxicola* (Schauf and Bullock, 1979, 1980, 1982) and squid axons (Meves, 1974). Nevertheless our data suggests that future work may be able to resolve and quantify small effects of D_2O on the kinetics of the slower components of gating current. We find no differences between the effects of internal (Fig. 2 *A*) and external (Fig. 2 *B*) D_2O application on gating current.

In Fig. 3 records of ionic current are shown at voltages of −20 mV (*A*), 0 mV (*B*), and +20 mV (*C*). Because D_2O decreases maximal sodium channel conductance (~20%), currents recorded in the solvent (traces *b* in each panel) have been scaled to the peak inward current magnitude of the record taken in H_2O (traces *a* in each panel) to aid visual comparison of the D_2O effects. We have quantified these effects for the voltage range −40 to +60 mV (see Table 1). The ratio of D_2O/H_2O was determined both for time to peak inward current magnitude (t_p) and the time to one-half peak current magnitude ($t_{1/2}$) in a series of six axons. Our results show this ratio as 1.31 ± 0.07 and 1.33 ± 0.18 for t_p and $t_{1/2}$, respectively. Ionic current was analyzed over an 8-ms time course, and we find that the asymptotic value for steady-state I_{Na} is not changed during exposure to D_2O. This is not readily apparent in Fig. 3 *A* where we show I_{Na} traces recorded at −20 mV and plotted on a short time base. However, at

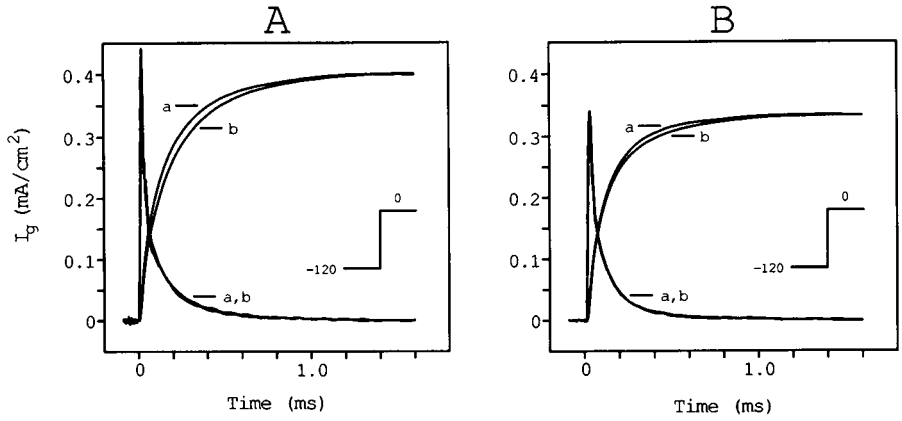

FIGURE 2 Gating currents are relatively insensitive to D_2O. Gating currents and corresponding integrations at 0 mV before (traces *a*) and during (traces *b*) internal (panel *A*) and external (panel *B*) D_2O perfusion. Integration of these gating current traces over a 2-ms period gives the following total gating charge movements: (*A*) trace *a*, 38; *b*, 37 nC/cm^2; (*B*) trace *a*, 31; *b*, 32 nC/cm^2. Holding potential, −120 mV. Data represented are from axons 890726, (D_2O, 20 Na//TTX, 50 Na), panel *A*, and 881118, (0 Na//D_2O, TTX, 0 Na), panel *B*.

the more positive voltages such as +20 mV (Fig. 3 *C*), where the kinetics are faster, it becomes more visible that the asymptotes are analogous in H_2O and D_2O. Thus our data confirms the major findings reported from *Myxicola* by Schauf and Bullock (1979). D_2O significantly slows activation and inactivation kinetics of I_{Na}, and this slowing action is voltage-insensitive (see Table 1).

Schauf and Bullock (1982) also reported that the sodium channel tail current was apparently insensitive to the solvent effects. They noticed that when the tail current records in H_2O and D_2O were scaled and superimposed, the fast components were identical while the slower components showed slight sensitivity or variability in D_2O. In Fig. 4 we show tail currents recorded at −80 mV after a test potential to +20 mV for 1 ms (see pulse pattern in Fig. 4 *A*; we plot only the portion of the current trace corresponding to the continuous line of this pulse diagram). Both the fast and slow kinetic components of the decaying tail current are clearly visible in these records. In Fig. 4 *A* we have scaled the D_2O record such that the slow components overlie; these records superimpose exactly with no detectable kinetic dissimilarity in their rates. Trace *a* was recorded in H_2O and trace *b* in D_2O. We then rescaled the D_2O record to match the control peak tail current (see Fig. 4 *B*). The fast components of these traces now overlie with no apparent dissimilarities in their rates. However, we also noticed (as did Schauf and Bullock [1982] from *Myxicola*) that when

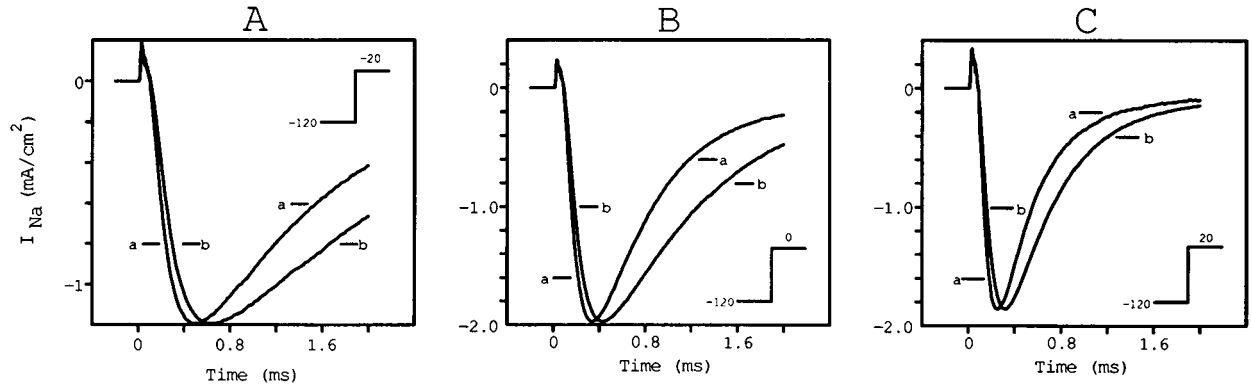

FIGURE 3 I_{Na} activation and inactivation kinetics are slowed by D_2O. Ionic currents before (traces *a*) and during external D_2O perfusion (traces *b*) are compared for voltages of −20 mV (*A*), 0 mV (*B*), and +20 mV (*C*). D_2O records (traces *b*) have been recorded with a higher external sodium concentration and then scaled to account for reduction in peak current magnitude. Holding potential, −120 mV. All data are from axon 881122, (0 Na//50 Na) in H_2O and (0 Na//D_2O, 100 Na) in D_2O.

TABLE 1 Effects of D_2O across voltage (V_m)

	Time to peak I_{Na} t_p		Time to ½ peak I_{Na} $t_{1/2}$		Ratio D_2O/H_2O	
V_m	H_2O	D_2O	H_2O	D_2O	t_p	$t_{1/2}$
mV	*μs*	*μs*	*μs*	*μs*		
−40	902* (1)	1,232 (1)	328 (1)	528 (1)	1.37	1.60
−20	531 ± 36.9 (6)	640 ± 17.6 (6)	219 ± 20.8 (6)	265 ± 13.5 (6)	1.21	1.21
0	391 ± 41.1 (4)	550 ± 76.8 (4)	156 ± 23.7 (4)	247 ± 49.3 (4)	1.41	1.58
20	256 ± 4.1 (3)	318 ± 10.3 (3)	128 ± 0 (3)	149 ± 4.62 (3)	1.24	1.16
40	208 (1)	278 (1)	106 (1)	128 (1)	1.34	1.21
50	174 ± 4.9	228 ± 6.1	84 ± 1.1 (3)	105 ± 14.1 (3)	1.31	1.25
60	174 (1)	226 (1)	90 (1)	114 (1)	1.30	1.27

*Values presented as mean ± SD and (*n*).

the fast components are scaled as in Fig. 4 *B*, reduction in the relative intercept of the slow component (trace *b*) in D_2O is more evident. We found a similar change at all prepulse durations investigated (0.4–6 ms).

Could series resistance errors be obscuring kinetic effects of D_2O on tail current kinetics? If the axon were markedly undercompensated in control conditions, reduction in peak tail current during exposure to D_2O could reduce the voltage error and so lead to an artifactual increase in deactivation kinetics. The artifactual voltage shift could mask a slowing by D_2O; this problem would be accentuated if D_2O reduced series resistance. We recognize that D_2O reduces the equivalent conductivity of electrolyte solutions (Swain and Evans, 1966) and thus would be expected to increase R_s, however series resistance may be markedly affected by other factors (such as osmotic changes in Schwann cells as well as inward vs. outward solvent fluxes [see Stimers et al., 1987; Alicata et al., 1989]). Thus other, less readily predictable changes might override the conductivity effect.

Schauf and Bullock (1982) were careful to recompensate their axons after exposure to D_2O. In our experiments we changed external sodium concentration to maintain approximate equivalence of peak currents before and after D_2O exposure. Additionally, we monitored R_s changes throughout the course of these experiments, using peak capacity current as the measured parameter (see Alicata et al., 1989). D_2O initially produces a small increase in R_s, but this increase disappears over time, and R_s is typically slightly reduced later in the experiment. Neither the peak magnitudes nor the kinetics of our tail currents were significantly affected by these small R_s changes. We therefore conclude that tail current kinetics are insensitive to D_2O.

Armstrong and Bezanilla (1974) and Keynes and Rojas (1976) (squid giant axon) and Hahin and Goldman

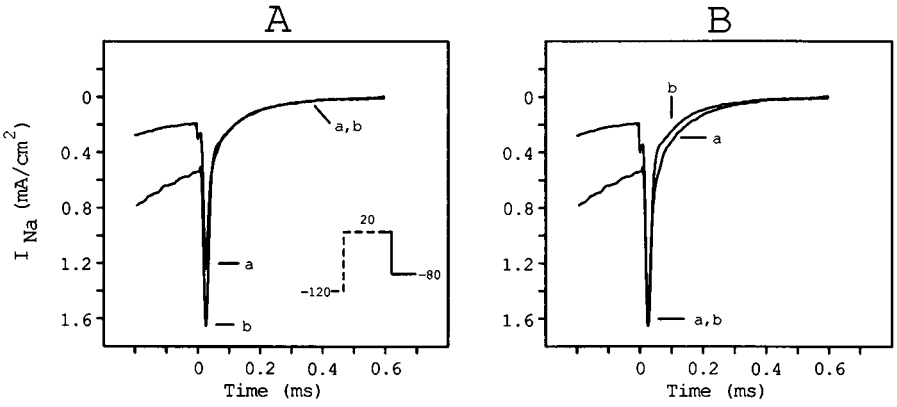

FIGURE 4 The rates of the fast and slow components of sodium channel tail current are not affected by D_2O. Tail currents at −80 mV after a depolarizing pulse of +20 mV for 1 ms are shown before (traces *a*) and during external D_2O perfusion (traces *b*). Data traces correspond to the continuous line of the pulse pattern insert shown in panel *A*. (*A*) D_2O trace has been scaled, such that the slow components overlie, to aid visual comparison of the rates. (*B*) Records from *A* were rescaled to the same peak tail current magnitude to compare the rates of the fast components. Holding potential, −120 mV. All data are from axon 881122, (0 Na//50 Na) in H_2O and (0 Na//D_2O, 100 Na) in D_2O.

(1978) and Bullock and Schauf (1978) (*Myxicola*) have observed that a conditioning prepulse alters the time-dependent onset ("Cole-Moore-type" shift) in sodium channel activation after a subsequent membrane depolarization (see pulse pattern *b* in Fig. 5, *B* and *C*). Schauf (1983) reported that although D_2O causes significant slowing of channel activation and inactivation, it was without effect on prepulse-dependent delays in channel activation visible after conditioning hyperpolarizing prepulses. Schauf had predicted this result on the premise that because D_2O was unable to alter gating current, which he presumed to arise from transitions between nonconducting precursor states, it would also have no affect on "Cole-Moore-type" shifts (which have also been supposed to arise from changes in relative occupancy of early preopen states [see Taylor and Bezanilla, 1983]).

Fig. 5 *A* shows the single pulse control records at 0 mV in H_2O and D_2O. The D_2O record is not scaled demonstrating that D_2O decreases maximum sodium conductance by ~20%. In Fig. 5 *B* we demonstrate the time shift of channel activation kinetics, in H_2O, after a conditioning depolarizing prepulse to −65 mV (trace *b*) by comparison with the single pulse record (trace *a*). Trace *b* was scaled to match the peak current of the single-pulse record to aid visual comparison of the shift in activation. We evaluated the "Cole-Moore-type" shift by determining the difference in $t_{1/2}$ between single-pulse and double-pulse records. In H_2O (Fig. 5 *B*) the shift in activation ($\Delta t_{1/2}$) is 20 μs. We repeated the above protocol in D_2O (Fig. 5 *C*) and found the magnitude of the "Cole-Moore-type" shift ($\Delta t_{1/2}$) to be 32 μs. At a different test potential of +50 mV the magnitude of the shift ($\Delta t_{1/2}$) in I_{Na} was 13.5 μs in H_2O and 17.0 μs in D_2O. Our results for the "Cole-Moore-type" shift experiments are summarized in Table 2. We noticed, at the two voltages tested, the magnitude of the prepulse-dependent shift in activation was ~1.4-fold greater in D_2O than in H_2O. However, when the magnitude of the shift is experssed as the ratio of $\Delta t_{1/2}/t_{1/2}$ (single-pulse), this ratio is not changed by D_2O. Thus our data confirms the results reported from *Myxicola* by Schauf (1983).

If sodium channel activation and inactivation are sequentially coupled processes, (Bezanilla and Armstrong, 1977; see also review by French and Horn, 1983), then a specific effect of D_2O on inactivation might affect activation only indirectly. Does D_2O slow I_{Na} activation kinetics after removal of fast inactivation with 10 mM chloramine-T (ch-T)? In Fig. 6 we show that the slowing effect of D_2O on activation kinetics remains after >90% of fast inactivation was removed with a single treatment of 10 mM ch-T (trace *d*). The control record (H_2O) following ch-T treatment is shown in trace *c*. For comparison we also provide records from the same axon before removal of fast inactivation, before (trace *a*) and during exposure to D_2O (trace *b*). In this axon the D_2O/H_2O ratios (cf Table 1) determined for t_p and $t_{1/2}$ at 0 mV are 1.41 and 1.36 where fast inactivation is intact and 1.41 and 1.36 after ch-T treatment. This evidence demonstrates that activation is the primary target site for the observed D_2O action on I_{Na} kinetics.

Oxford (1981) showed that when a maintained depolarization was interrupted by a brief return (~100 μs) to holding potential (see Fig. 7 *A*, pulse pattern inset), reactivation turns on rapidly with almost monoexponential kinetics. He referred to this faster activation process as secondary activation. When the interpulse interval was

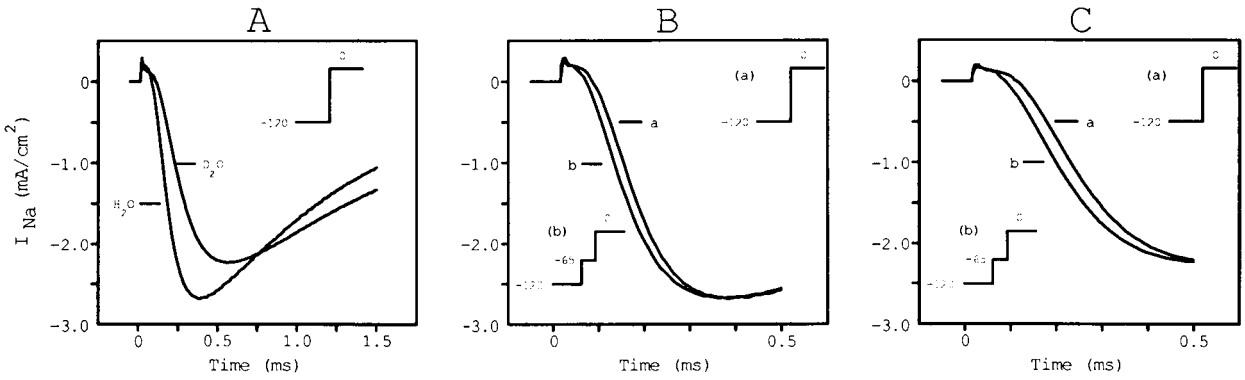

FIGURE 5 D_2O does not affect the relative magnitude of the prepulse-induced "Cole-Moore-type" shifts in channel activation. (*A*) Ionic current at 0 mV in H_2O and D_2O. Traces were not scaled to illustrate the D_2O-induced slowing of activation and inactivation kinetics and the decrease in sodium conductance. Holding potential, −120 mV. Ionic current at 0 mV in H_2O (*B*) and D_2O (*C*) after a single pulse (traces *a*) and a 5-ms prepulse to −65 mV (traces *b*). Current records resulting from the prepulse (traces *b*) were scaled to peak current magnitude of the single pulse record (traces *a*) for comparison of the "Cole-Moore-type" shifts in channel activation. The "Cole-Moore-type" shifts are 20 μs for H_2O in *B* and 32 μs for D_2O in *C* but the ratio $\Delta t_{1/2}/t_{1/2}$ (single pulse) is not altered by solvent substitution (see Table 2). All data are from axon 880928b, (20 Na//80 Na) in H_2O and (20 Na//D_2O, 100 Na) in D_2O.

TABLE 2 Comparison of "Cole-Moore-type" shifts in H_2O and D_2O at 0 and 50 mV

	0 mV		+50 mV	
Time (μs)	H_2O	D_2O	H_2O	D_2O
$t_{1/2}$ single pulse	174.0	244.0	94.0	123.5
$t_{1/2}$ double pulse	154.0	212.0	80.5	106.5
$\Delta t_{1/2}$ "C-M shift"*	20.0	32.0	13.5	17.0
$\Delta t_{1/2}/(t_{1/2}$ single pulse)	0.12	0.13	0.14	0.14

*$\Delta t_{1/2} = t_{1/2}$ single pulse $- t_{1/2}$ double pulse.
Data from axon 880928b.

progressively increased, secondary activation increasingly assumed the sigmoidal appearance of primary activation. We were interested to see whether primary and secondary activation were equally sensitive to the slowing effects of D_2O. In Figs. 7 and 8 we show results obtained using this double-pulse protocol. All experiments were performed after treatment with 10 mM ch-T. Fig. 7 *A* shows secondary activation obtained after an interpulse interval of 50 μs (trace *b*). In crayfish axons, as in Oxford's squid axons, secondary activation turns on very fast without the usual sigmoid kinetics shown in the single pulse record (trace *a*). However, when interpulse interval is increased to 400 μs (Fig. 7 *B*, trace *b*), the reactivation process nearly overlies the sigmoid primary activation kinetics shown in the single pulse control record (Fig. 7 *B*, trace *a*).

Fig. 8 *A* shows I_{Na} records obtained from the double-pulse protocol (in both H_2O and D_2O) with a 50-μs interpulse interval. Secondary activation in H_2O and D_2O are indistinguishable and D_2O appears to have no affect

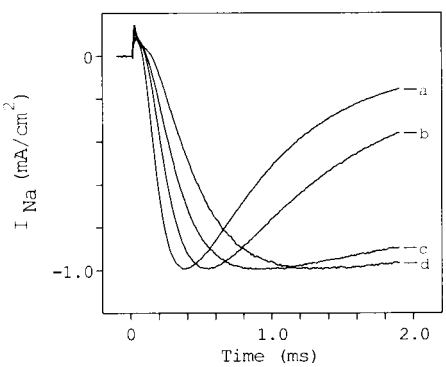

FIGURE 6 D_2O slows sodium channel activation kinetics after removal of fast inactivation by 10 mM chloramine-T. Ionic current with inactivation intact at 0 mV before (trace *a*) and during internal D_2O perfusion (trace *b*). Holding potential, −120 mV. Ionic current at 0 mV before (trace *c*) and during internal D_2O perfusion (trace *d*) after <90% of fast inactivation was removed by prior treatment with 10 mM chloramine-T. Holding potential, −90 mV. All records were scaled to ~1 mA/cm² current magnitude for comparison of activation kinetics. All data from axon 890608, (D_2O, 20 Na//75 Na).

on this component of activation. On the other hand, primary activation is markedly slowed by D_2O. After an interpulse interval of 400 μs (Fig. 8 *B*) the kinetics and D_2O sensitivity of secondary activation return towards those of primary activation. The D_2O insensitivity of secondary activation after brief (50 μs) interpulse intervals will be further considered in the Discussion section.

In this series of experiments we have been careful to repeat all major observations with both internal and external D_2O perfusion. We have noted no qualitative or quantitative differences resulting from method of solvent application other than (see Methods) a marked negative effect on axon survival when D_2O is applied externally. The similar effects of internal and external D_2O application may be seen for gating current (compare Fig. 2, *A* and *B*), for ionic current activation (compare Figs. 3 and 6) and for tail currents (compare Figs. 1 *A* and 4).

DISCUSSION

The principal results of this study are: (*a*) D_2O slows sodium channel activation and inactivation (Figs. 3 and 5 *A*) without significantly affecting the kinetics of I_gON, I_gOFF (Figs. 1 *B* and 2), sodium tail currents (Fig. 4) or the relative magnitude of prepulse-induced "Cole-Moore-type" shifts (Fig. 5). (*b*) Similar results were obtained with both internal and external D_2O perfusion (compare Figs. 2, *A* and *B*, for gating current, Figs. 3 and 6 for ionic current activation, Figs. 1 *A* and 4 for tail currents, recorded during internal and external perfusion, respectively). (*c*) Removal of fast inactivation with chloramine-T did not affect the results obtained during D_2O perfusion (Fig. 6). (*d*) The double-pulse protocol demonstrates that secondary activation, after a brief (50 μs) interpulse interval, is not affected by D_2O (Figs. 7 and 8).

In many respects our experimental results in crayfish axons confirm those of previous investigators using other preparations. Conti and Palmieri (1968) noted that sodium currents in squid giant axons were slowed by ~1.4-fold after exposure to D_2O. Subsequently Meves (1974) showed that gating currents were unaffected by D_2O although tail sodium current was apparently slowed (~1.4-fold). Schauf and Bullock (1979) similarly noted no effect of D_2O on gating currents, although both sodium activation (measured as time-to-peak) and sodium inactivation (measured as τ_h) were both slowed by 1.4-fold at 6°C. However, this slowing was significantly temperature dependent, being almost eliminated at 16–18°C. Their least-squares fit for time-to-peak data showed the D_2O/H_2O ratio = $1.68 - 0.038T$, where T is temperature in degrees Celsius. This equation predicts a ratio of 1.32 for our data in Table 1 (at 9.5°C), which compares well with

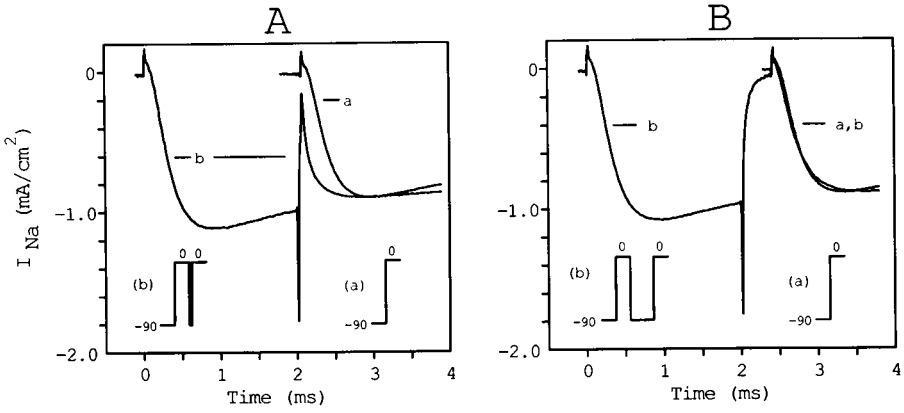

FIGURE 7 Double-pulse protocol (Oxford, 1981) reveals a component of activation which turns on very rapidly with almost monoexponential kinetics. (*A*) Ionic current at 0 mV after a control single pulse (trace *a*) and a double pulse interrupted by a 50 μs return to holding potential (trace *b*). (*B*) Ionic current at 0 mV after a control single pulse (trace *a*) and a double pulse interrupted by a 400-μs interpulse interval (trace *b*). For comparison of activation kinetics the single pulse (traces *a*, *A* and *B*) is superimposed on the I_{Na} record associated with the second pulse of a double pulse protocol (traces *b*, *A* and *B*). See pulse inset. Holding potential, −90 mV. Records were obtained after treatment with 10 mM chloramine-T. All data from axon 890608, (D_2O, 20 Na//75 Na).

the 1.31 ± 0.07 found for our results. Thus, quantitatively similar kinetic actions of D_2O have now been reported from squid, *Myxicola,* and crayfish axons.

Schauf and Bullock (1982) extended their study of D_2O actions to include tail current deactivation. In a series of six axons they found no significant effects on either the fast or slow kinetic components of I_{Na} tails. This result seems in direct conflict with Meves (1974) observation, from a more limited series of experiments, that I_{Na} tail current was slowed by D_2O. We have carefully repeated the tail current experiments and exactly confirm the data obtained by Schauf and Bullock. Furthermore, we are now able to explain the slight discrepancy in the slow tail current component noted in their scaled data (see Fig. 3 *b* of Schauf and Bullock, 1982). As seen in our Fig. 4 *B*, when control and D_2O records are scaled to the same peak tail current magnitude, the slow components no longer overlie because we note that there is a shift in the relative intercept of the slow tail component after exposure to D_2O but no change in kinetics of either component.

Our work summarized above provides additional support for two major conclusions presented by Schauf and Bullock (1979, 1982): *First,* activation and fast inactivation of sodium current are both slowed by D_2O without marked effects on gating current kinetics. This observa-

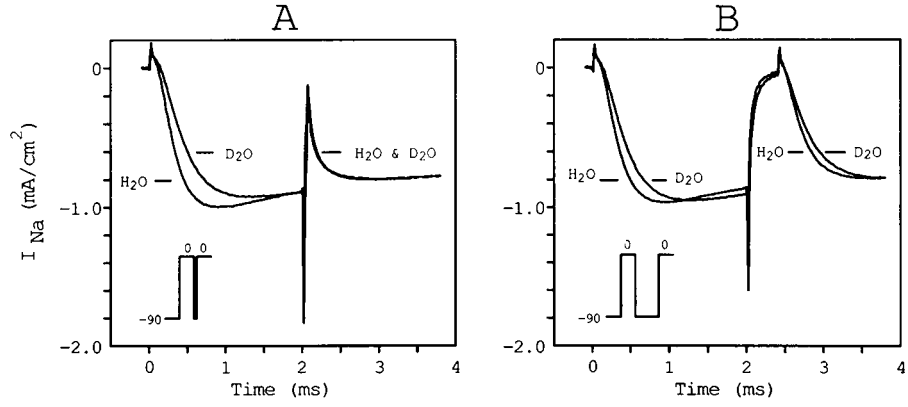

FIGURE 8 Secondary activation is insensitive to the slowing effects of D_2O. Ionic current at 0 mV before and during internal D_2O perfusion are shown after a double-pulse protocol with interpulse intervals of 50 μs (*A*) and 400 μs (*B*). Traces in H_2O and D_2O are superimposed in *A* and *B* to facilitate comparison of activation kinetics. Holding potential, −90 mV. Records were obtained after treatment with 10 mM chloramine-T. All data from axon 890608, (D_2O, 20 Na//75 Na).

tion demonstrates that relatively little gating charge movement (or inherent voltage sensitivity) can be associated with the final channel opening transition (see Appendix). *Second,* because D_2O slows activation but not tail current deactivation, it follows that some fundamental difference must exist between the channel gating mechanisms responsible for activation and tail current deactivation.

The first conclusion is qualitatively consistent with results of previous electrophysiological studies despite the apparent conflict with recent structural work (see Introduction). Although sequential models have usually placed a valence of $>1e$ in the final channel opening step (see Armstrong and Bezanilla, 1977; Bezanilla and Armstrong, 1977; Stimers et al., 1985), this is markedly less than the total valence of the preceding closed state transitions. Neumcke et al. (1976), Bullock and Schauf (1978), Armstrong (1981), as well as French and Horn (1983) have commented that the major component of gating charge movement precedes the major increase in sodium conductance. Thus the final channel-opening step(s) have been presumed to make only small contributions to total charge movement. Changes in the rates of such slow, low-valence transitions would be difficult to detect in gating current records. Although the gating currents of Fig. 2 appear almost identical, slight differences are visible in the integration traces for the crucial time zone (between 0.2 and 0.8 ms), where the largest kinetic changes would be expected.

By contrast, the second of Schauf and Bullock's conclusions (see above) has met with little acceptance, despite the precision of the tail current records provided by Schauf and Bullock (1982). There is, inevitably, an apparent internal contradiction in data which shows D_2O-induced dissociation between gating current and channel opening without an equivalent dissociation during channel deactivation. More significantly, Oxford (1981) carefully examined reactivation (secondary activation) after return steps to holding potential of differing durations imposed during depolarizing pulses. Brief return steps to holding potential, which should catch channels in closed states adjacent to the open state, demonstrated secondary activation with rapid, almost monoexponential, kinetics. He therefore concluded that deactivation occurs via reversal of the normal multi-step activation pathway (Scheme 1), rather than through an alternative direct path which bypasses intermediate closed states, as initially suggested by Bezanilla and Armstrong (1975*a* and *b*) (Scheme 2).

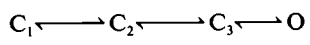

Scheme 1

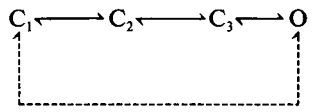

Scheme 2

Oxford's study has provided major support for models in which activation is considered as a linear sequential process (see review by French and Horn, 1983). For example, none of the 25 models tested statistically by Horn and Vandenberg (1984) considered the possibility of deactivation by a separate pathway (other than via reversal of the C_3-to-O activation step). However, this conclusion that deactivation is the reverse of primary activation appears to be in direct conflict with Schauf and Bullock's (1982) conclusion that activation and deactivation must utilize different pathways.

Despite the contradictory conclusions reached in these studies, both the secondary activation data of Oxford (1981) and the tail current data of Schauf and Bullock (1982) have been successfully repeated in crayfish axons. For short interpulse intervals secondary activation shows rapid, nearly monoexponential, rates (Fig. 7 *A*). However, D_2O slows the kinetics of primary activation (Fig. 3 and Table 1) without affecting tail current kinetics (Fig. 4).

This apparent paradox may be resolved by the experiment shown in Fig. 8, which assesses the effect of D_2O on secondary activation. We find that secondary activation, like tail current deactivation, is insensitive to D_2O (see Fig. 8 *A*). We conclude that D_2O-insensitive tail current deactivation cannot be the reverse of the D_2O-sensitive step responsible for channel opening during primary activation. However, D_2O-insensitive secondary activation may well represent reversal of the D_2O-insensitive tail current deactivation step. Oxford's (1981) observations can thus be reinterpreted as indicating that the deactivation path, like the primary activation path, involves a multistep reaction sequence. When the interpulse interval is in the order of 50–100 μs, many channels appear to have been caught no further than one reaction step away from the open state. However, these channels may well be following a different D_2O-insensitive pathway (just as Schauf and Bullock [1982] concluded).

The results noted above appear to rule out the standard linear activation mechanism (Scheme 1) in favor of a cyclical activation model shown by Scheme 3 (see Appendix).

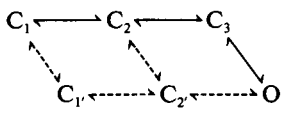

Scheme 3

In our schematics, left-right distance has been used to indicate distance moved through the transmembrane field. Thus, in Scheme 3, we presume the reaction C_1 to C_2 shows greater voltage sensitivity than the inherently slower C_1 to C_1' step. Hence the upper pathway can dominate primary activation during large depolarizing pulses. Similarly, in return pulses to negative holding potentials, the fast O to C_2' step will dominate the deactivation process. We suggest that the reversal of this reaction generates the rapid kinetics of secondary activation. On the other hand, at potentials > -40 mV in stationary microscopic analyses, deactivation could well occur principally via the O to C_3 step. We presume that this slower reaction step is the primary D_2O-sensitive transition.

Structural implications of the cyclical activation model

We recognize three alternative physical interpretations of the Scheme 3 model. *First,* three separate gating "particles" (or S4 segments) with differing effective valences might act as parallel activation gates (Guy and Seetharamulu, 1986; Catterall, 1986). In this model the two paths would result from asymmetry introduced by the markedly lower valence of at least one S4 segment (see Appendix). The relative insensitivity of ON gating current to D_2O would here result from the markedly lesser voltage sensitivity of the lower valence S4 particle. Furthermore, if channel "gating" requires that a charge must pass close to the solvent phase, the most D_2O-retarded transition might well be that of the least "voltage-driven" particle.

Second, two particles might operate as parallel activation gates. Again the asymmetry would arise from unequal particle valences, with the higher valence particle crossing the membrane field in several sequential steps, as suggested by Fohlmeister and Adelman (1985). In this model the steps do not necessarily cross equal fractions of the total field, nor are their apparent rates predictable other than by careful experimentation.

It should be noted that both these models assume a final slow primary activation step, generated by the slower low valence particle. This assumption explains the D_2O-sensitive delay in activation, without significant change in I_g kinetics, as seen here (Fig. 1) and also by Schauf and Bullock (1979). Thus the assumption that S4 segments have direct channel gating properties (see Introduction) seems consistent with the additional physiological evidence provided in this study, particularly in view of the very rapid kinetics of secondary activation.

Third, a single high valence gating particle might move through the membrane field following physically distinct alternative paths which are energetically favored under different conditions. Visualizing the mobile particle as a "helical screw" (Guy and Seetharamulu, 1986) it could screw "in" and "out" by reversing rotational directions (the primary activation path), or it could "jump the threads" and return to the starting position without reversing its direction of rotation (the secondary activation and tail current path). Intermediate energy barriers might be quite different along these two pathways.

In either case, Scheme 3 may be a substantial simplification of the full-state diagram, permissible only when discussing the effects of large voltage steps (see Appendix). However these models would seem to be potentially experimentally differentiable. For example, the first two models are necessarily kinetically symmetrical such that the C_1-to-C_2 and C_1-to-C_2' rates must be identical at given potential. By contrast the third model faces no such restrictions because barrier heights, and even barrier numbers, may be different for each pathway. Further studies will be required to distinguish between these possibilities. Recent work (Stühmer et al., 1989) has shown that site-directed modification of the S4 segment of domain I alters the effective valence of the sodium channel. However, similar changes in domain II produced little change in channel valence. Thus, at least one S4 segment may not be significantly involved in control of channel activation.

APPENDIX: MODEL SIMULATIONS

We demonstrate here that the principal conclusions reached in this study are consistent with the results of model simulations. Our models, like Schemes 1–3 (see Discussion), do not include inactivation. The simulations shown here may thus be compared to our data after removal of inactivation with chloramine-T (see Figs. 6–8).

Modeling methods and procedures

For each model all transitions were specified in accordance with Eyring rate theory (Glasstone et al., 1941; Woodbury, 1971; Stimers et al., 1985) such that the rate constants $K_{i,j}$ and $K_{j,i}$ are:

$$K_{i,j} = (kT/h) \exp(-W_i - ez'xV/kT)$$

$$K_{j,i} = (kT/h) \exp(-W_j + ez'(1-x)V/kT),$$

where W is the height of the energy barrier (in kT units) as seen from well i or j, respectively, e is the electronic charge, z' is the effective valence of the i,j transition, x is the fraction of the distance between wells i and j at which the barrier peak occurs, V is the membrane potential, k is the Boltzmann constant, T is the absolute temperature, and h is the Planck constant. No electrostatic interactions between adjacent transitions (see Bezanilla et al., 1982; Stimers et al., 1985; Rayner and Starkus, 1989) have been assumed in the model simulations shown here.

Simulations were carried out using a Sun 3/60 (Sun Microsystems, El Segundo, CA). Our modeling program employs simple Euler integration to solve the array of simultaneous equations representing the allowed transitions within each particular model formulation. Cumulative errors were <0.001% at the end of each model run. All "ionic current" simulations, including tail current deactivations, are presented

as changes in "fractional conductance." Also all voltage steps were presumed instantaneous, such that the fast component of the simulated gating currents necessarily seems exaggerated by comparison with experimental records taken at finite clamp speeds. Holding potential was presumed to be −120 mV for each simulation, and calculated initial state occupancies were used for each model run.

Modeling strategies

We find that the most successful simple linear (Scheme 1) models are those comprising three "reactions" with characteristically different valences and kinetics; the "fast," "intermediate," and "slow" reactions. To mke it easer to follow the effects of changes in reaction order (Fig. 9) and particle number (Fig. 10) we have kept reaction parameters reasonably constant from model to model. For example, in each model the major valence remains associated with the "intermediate" step (yielding acceptable gating current waveforms for all models), whereas the "slow" reaction is always the D_2O-sensitive step.

We have maintained this approach while exploring the cyclic models of Schemes 2 and 3, although the physical mechanism which these "reactions" represent necessarily changes from model to model. Thus for the linear Scheme 1 models, each reaction represents one sequential step of a single gating particle. By contrast for Scheme 3, each reaction may represent either one of three independent parallel gating particles (as in the eight-state version [see Fig. 10 *C*]), or two sequential steps of one particle plus a second independent particle (as in the six-state

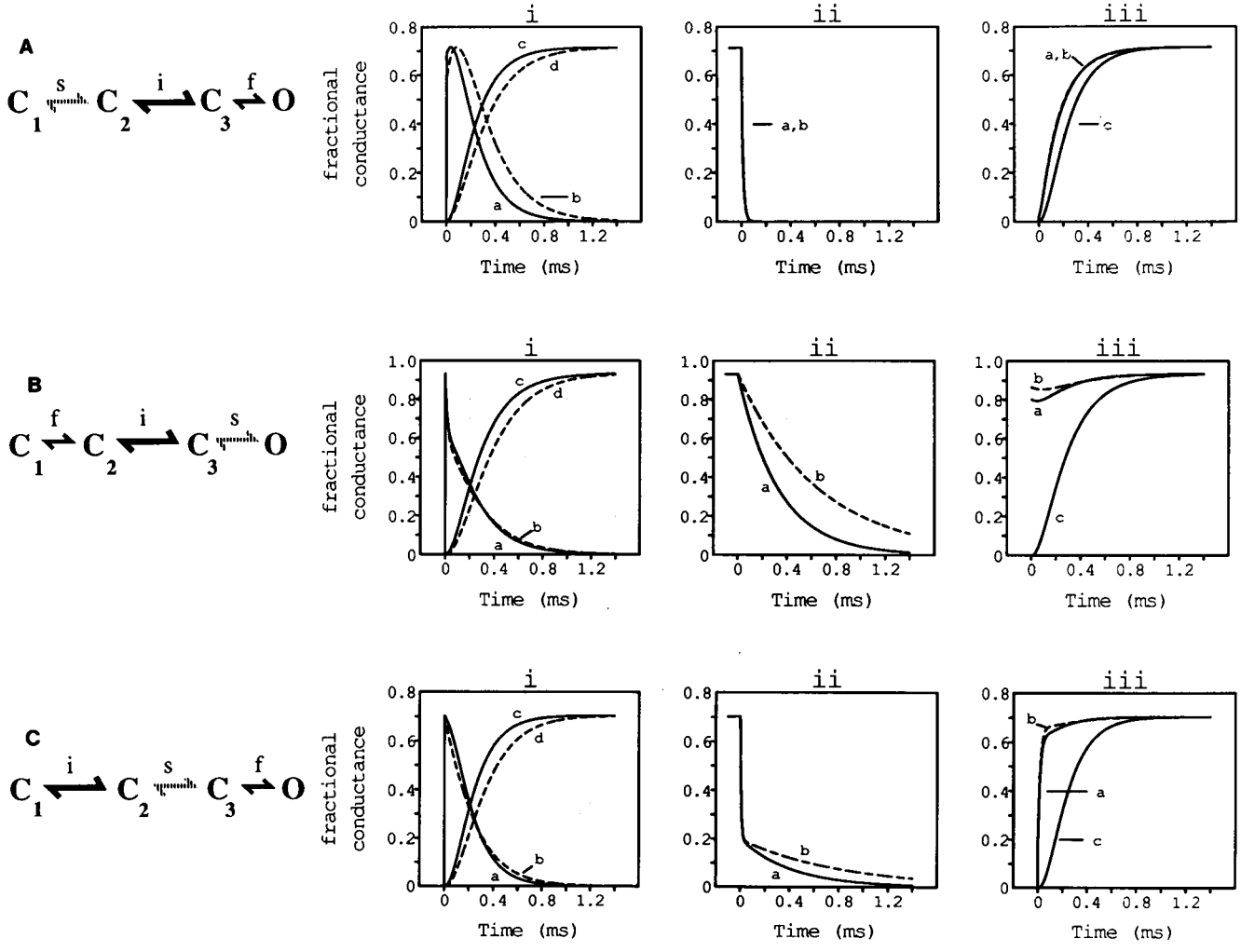

FIGURE 9 Simulations of three simple, Scheme 1, linear activation models (*A*, *B*, and *C*) do not satisfy our evaluation criteria (see Appendix). For each model, panel *i* shows gating current (trace *a*, control; trace *b*, D_2O) and ionic current simulations (trace *c*, control; trace *d*, D_2O) for primary activation during a voltage step from −120 mV holding potential to +20 mV test potential; panel *ii* shows channel deactivation (trace *a*, control; trace *b*, D_2O) associated with a return step to holding potential following a 2-ms pulse to +20 mV test potential; panel *iii* shows secondary activation (trace *a*, control; trace *b*, D_2O) after a 50-μs return to holding potential imposed during a depolarizing step to +20 mV test potential. These secondary activation traces are compared with control primary activation rate (trace *c*). For each panel, abscissa is time in microseconds; ordinate is fractional conductance (simulated gating currents have been normalized to peak sodium conductance in each model). Cartoons show reaction order where *f* indicates the "fast" reaction (*short arrow*), *i* indicates the "intermediate" reaction (*heavy arrow*) and *s* shows the "slow" D_2O-sensitive reaction (*dashed arrow*). In each model the effects of D_2O were simulated by approximately halving the rates of the slow reaction step (see Table 3).

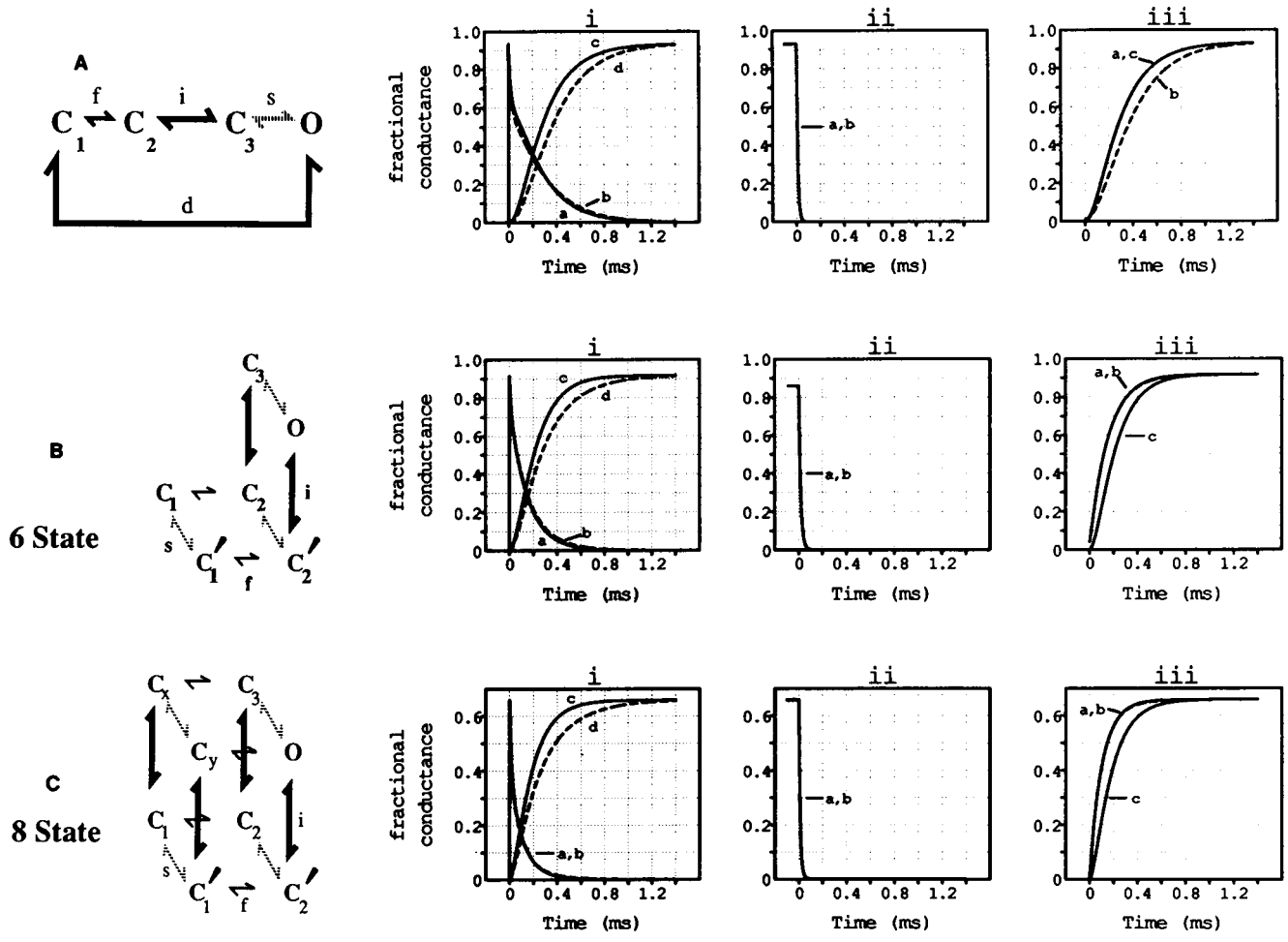

FIGURE 10 Simulations using the simple Scheme 2 cyclical model (*A*) do not satisfy our evaluation criteria (see Appendix). By contrast, both the six-state (*B*) and eight-state (*C*) versions of the Scheme 3 are cyclical model produce fully acceptable simulations. Model parameters are given in Table 3; simulation parameters for each panel are the same as for Fig. 9. Cartoons indicate models used (see Fig. 9 for explanation of symbols); note, however, the additional deactivation reaction *d* present only in the Scheme 2 model (*A*). Nomenclature used for channel states is the same as that used for Schemes 1–3 (see Discussion), except that two additional states (states C_x and C_y) are required for the eight-state Scheme 3 formulation.

version [see Fig. 10 *B*]). Finally, reaction parameters (see Table 3) have been selected to achieve reasonable fits to additional criteria (such as the voltage sensitivities of activation and deactivation kinetics) not used for evaluation here (see below). In each model the effects of D_2O were simulated by approximately halving the rates of the "slow" reaction (see Table 3), giving a 1.3-fold slowing of $t_{1/2}$ activation for all models.

Evaluation criteria

All models were evaluated against the following major criteria (for which fit could be assessed without model by model parameter optimization): (*a*) D_2O slows channel activation without significant effects on gating current. (*b*) Tail currents (at −120 mV) are fast compared with channel activation kinetics at +20 mV test potential. Furthermore the intercept of the slow tail current component, after removal of fast inactivation, is no more than ~10% of maximum sodium conductance (see Fig. 7 *B* and Hahin, 1988). (*c*) Both fast and slow tail current components are insensitive to D_2O. (*d*) Secondary activation, after a brief interpulse interval, is fast by comparison with control primary activation rate. (*e*) Secondary activation is insensitive to D_2O.

Scheme 1 models

Model A

In this model the reaction order is "slow-intermediate-fast." As shown in Fig. 9 *A*, panels *ii* and *iii*, the fast final opening step gives fast deactivation and secondary activation kinetics which are not significantly D_2O-sensitive. In panel *iii*, secondary activation in D_2O (*dashed curve*, trace *b*) almost exactly overlies the control secondary activation (trace *a*). Both these curves are substantially faster than the control primary activation rate shown by trace *c*. However (see panel *i*), for the reaction order used in this model, the gating currents are necessarily delayed by D_2O-induced slowing of channel activation (*dashed curves*, traces *b* and *d*) in comparison with control activation kinetics (*solid curves*, traces *a* and *c*).

TABLE 3 Parameters for model simulations

A. Scheme 1 and Scheme 2 models Reaction	w_i	w_j	z'	x
Fast	18.8	19.4	0.4	0.2
Intermediate	21.0	24.0	1.8	0.3
Slow	20.5	22.5	0.8	0.7
D_2O-slow	21.2	23.2	0.8	0.7
Deactivation*	26.5	32.1	3.0	0.05
B. Scheme 3 models **Reaction**	w_i	w_j	z'	x
Fast	18.8	19.4	0.4	0.8
Intermediate	20.5	25.0	1.8	0.25
Slow	21.2	23	0.8	0.7
D_2O-slow	21.7	23.5	0.8	0.7

*Scheme 2 model only.

Model B

The reaction order here is "fast-intermediate-slow." As shown in Fig. 9 *B*, panel *i*, this order gives D_2O-induced slowing of channel activation (compare traces *c* and *d*) with only minor changes in gating currents (traces *a* and *b*). However, the slow D_2O-sensitive final step gives slow D_2O-sensitive tail currents (see panel *ii*, trace *b*) with reduced, slow, secondary activation (see panel *iii*, traces *a* and *b*).

Model C

Here the reaction order is "intermediate-slow-fast." We had reasoned that this sequence might show both the tail currents and secondary activation of model A, coupled with the lack of effect of D_2O on gating current kinetics seen in model B. Fig. 9 *C*, panel *i*, shows that gating currents are not particularly D_2O-sensitive. However, the tail currents (see panel *ii*) show a prominent slow D_2O-sensitive component, whereas secondary activation fails to show the near monoexponential kinetics seen for model A in Fig. 9 *A*, panel *iii*, traces *a* and *b*. Although the kinetics of secondary activation improved after a twofold slowing of the fast reaction (not shown), this change did not affect the intercept or D_2O-sensitivity of the slow tail current component shown in Fig. 9 *C*, panel *ii*.

The scheme 2 model

Oxford's study (1981), which includes computer simulations, makes clear that Scheme 2 models are incapable of generating the observed rapid secondary activation kinetics after brief interpulse intervals. Fig. 10 *A*, panel *iii*, demonstrates that this conclusion remains true for the reaction parameters used in our simulations. Note that trace *a* (control secondary activation) overlies trace *c* (control primary activation), whereas trace *b* (secondary activation after D_2O) is here the slowest activation kinetic.

Our formulation assumed a single gating particle activating via the sequence of steps from C_1 through C_2 and C_3 to O. The reaction order used for Fig. 10 *A* was "fast-intermediate-slow." However, we presume that an alternative direct pathway is available (between C_1 and O) which bypasses the intermediate energy barriers of this reaction sequence. Clearly this alternative path must show an effective valence equal to the sum of the valences of the primary activation path, while the difference between its energy wells must also be the same as the sum of the energy wells in the sequential path. In this model the alternative path is preferentially selected in repolarizing (but not depolarizing) voltage steps, due to the highly asymmetric barrier position for this reaction (see Table 3 *A*).

This model can be adjusted to give rapid secondary activation by adding an additional state (or states) along the alternative (O to C_1) deactivation pathway. However such modification makes this model identical with our "single particle" interpretation of the Scheme 3 model (see Discussion).

Scheme 3 models

The "single-particle" and "two-particle" interpretations of the Scheme 3 model can be fully represented by our six-state schema. As shown in Fig 10 *B*, this model meets all of our evaluation criteria. On the other hand, a "three-particle" model requires an eight-state formulation, as shown in Fig. 10 *C*. Conti and Stühmer (1989) have provided evidence from fluctuation analysis of gating current records, suggesting the presence of three separate gating particles. They note that one 1.8*e* particle together with two lower valence particles could be consistent with their data. Such a model also satisfies our evaluation criteria (see Fig. 10 *C*). Parameters for these models are shown in Table 3 *B*.

Summary

In conclusion: (*a*) The observed lack of effect of D_2O on I_gON kinetics indicates that the major gating current generating steps must precede the principal D_2O-sensitive transition (as suggested by Schauf and Bullock, 1979, 1982). (*b*) No simple linear model satisfies our evaluation criteria. (*c*) The simple Scheme 2 cyclical model fails to demonstrate rapid secondary activation (as noted by Oxford, 1981). (*d*) Models based on the cyclical system shown in Scheme 3 satisfy all evaluation criteria, regardless of whether a one-particle, two-particle, or three-particle formulation is used.

We thank Dr. Peter Ruben for his helpful comments and Richard Foulk for his programming assistance.

This work was supported by the National Institutes of Health through both research grant NS21151 (to J. G. Starkus) and RCMI award 3G12RR03061. Additional support was received from the American Heart Association (Hawaii Affiliate), the University of Hawaii Research Council, and BRSG 2S07 RR07026 awarded by the Biomedical Research Support Grant Program, Division of Research Resources, National Institutes of Health.

Received for publication 18 September 1989 and in final form 21 December 1989.

REFERENCES

Alicata, D. A., M. D. Rayner, and J. G. Starkus. 1989. Osmotic and pharmacological effects of formamide on capacity current, gating current, and sodium current in crayfish giant axons. *Biophys. J.* 55:347–353.

Armstrong, C. M. 1981. Sodium channels and gating currents. *Physiol. Rev.* 61:644–683.

Armstrong, C. M., and F. Bezanilla. 1974. Charge movement associated with the opening and closing of the activation gates of the Na channels. *J. Gen. Physiol.* 63:533–552.

Armstrong, C. M., and F. Bezanilla. 1977. Inactivation of the sodium channel. II. Gating current experiments. *J. Gen. Physiol.* 70:567–590.

Bezanilla, F., and C. M. Armstrong. 1975*a*. Kinetic properties and inactivation of the currents of sodium channels in squid axons. *Philos. Trans. R. Soc. Lond. B Biol. Sci.* 270:449–458.

Bezanilla, F., and C. M. Armstrong. 1975*b*. Properties of the sodium channel gating current. *Cold Spring Harbor Symp. Quant. Biol.* 40:297–304.

Bezanilla, F., and C. M. Armstrong. 1977. Inactivation of the sodium channel. I. Sodium current experiments. *J. Gen. Physiol.* 70:549–566.

Bezanilla, F., R. E. Taylor, and J. M. Fernandez. 1982. Distribution and kinetics of membrane dielectric polarization. 1. Long-term inactivation of gating currents. *J. Gen. Physiol.* 79:21–40.

Bullock, J. O., and C. L. Schauf. 1978. Combined voltage-clamp and dialysis of *Myxicola* axons: behavior of membrane asymmetry currents. *J. Physiol. (Lond.).* 278:309–324.

Catterall, W. A. 1986. Voltage-dependent gating of sodium channels: correlating structure and function. *TINS Trends Neurosci.* 9:7–10.

Conti, F., and G. Palmieri. 1968. Nerve fiber behavior in heavy water under voltage clamp. *Biophysik.* 5:71–77.

Conti, F., and W. Stühmer. 1989. Quantal charge redistributions accompanying the structural transitions of sodium channels. *Eur. Biophys. J.* 17:53–59.

Fohlmeister, J. F., and W. J. Adelman. 1985. Gating current harmonics. II. Model simulations of axonal gating currents. *Biophys. J.* 48:391–400.

French, R. J., and R. Horn. 1983. Sodium channel gating: models, mimics, and modifiers. *Annu. Rev. Biophys. Bioeng.* 12:319–356.

Glasstone, S., K. J. Laidler, and H. Eyring. 1941. The Theory of Rate processes. McGraw-Hill Book Co., New York. 522–599.

Guy, H. R., and P. Seetharamulu. 1986. Molecular model of the action potential sodium channel. *Proc. Natl. Acad. Sci. USA.* 83:508–512.

Hahin, R. 1988. Removal of inactivation causes time-invariant sodium current decays. *J. Gen. Physiol.* 92:331–350.

Hahin, R., and L. Goldman. 1978. Initial conditions and the kinetics of the sodium conductance in *Myxicola* giant axons. I. Effects on the time course of the sodium conductance. *J. Gen. Physiol.* 72:863–878.

Horn, R., and C. A. Vandenberg. 1984. Statistical properties of single sodium channels. *J. Gen. Physiol.* 84:505–534.

Huang, J. M., J. Tanguy, and J. Z. Yeh. 1987. Removal of sodium inactivation and block of sodium channels by chloramine-T in crayfish and squid giant axons. *Biophys. J.* 52:155–163.

Keynes, R. D., and E. Rojas. 1976. The temporal and steady-state relationships between activation of the sodium conductance and movement of the gating particles in the squid giant axon. *J. Physiol. (Lond.).* 255:157–189.

Meves, H. 1974. The effect of holding potential on the asymmetry currents in squid giant axons. *J. Physiol. (Lond.).* 243:847–867.

Neumcke, B., W. Nonner, and R. Stämpfli. 1976. Asymmetrical displacement current and its relation with activation of the sodium current in the membrane of frog myelinated nerve. *Pfluegers Arch. Eur. J. Physiol.* 363:193–203.

Noda, M., S. Shimizu, T. Tanabe, T. Takai, T. Kayano, T. Ikeda, H. Takahashi, H. Nakayama, Y. Kanaoka, N. Minamino, K. Kangawa, H. Matsuo, M. A. Raftery, T. Hirose, S. Inayama, H. Hayashida, T. Miyata, and S. Numa. 1984. Primary structure of *Electrophorus electricus* sodium channel deduced from cDNA sequence. *Nature (Lond.).* 312:121–127.

Oxford, G. S. 1981. Some kinetic and steady-state properties of sodium channels after removal of inactivation. *J. Gen. Physiol.* 77:1–22.

Rayner, M. D., and J. G. Starkus. 1989. The steady-state distribution of gating charge in crayfish giant axons. *Biophys. J.* 55:1–19.

Schauf, C. L. 1983. Insensitivity of activation delays in potassium and sodium channels to heavy water in *Myxicola* giant axons. *J. Physiol. (Lond.).* 337:173–182.

Schauf, C. L., and J. O. Bullock. 1979. Modifications of sodium channel gating in *Myxicola* giant axons by deuterium oxide, temperature, and internal cations. *Biophys. J.* 27:193–208.

Schauf, C. L., and J. O. Bullock. 1980. Solvent substitution as a probe of channel gating in *Myxicola*. Differential effects of D_2O on some components of membrane conductance. *Biophys. J.* 30:295–306.

Schauf, C. L., and J. O. Bullock. 1982. Solvent substitution as a probe of channel gating in *Myxicola*. Effects of D_2O on kinetic properties of drugs that occlude channels. *Biophys. J.* 37:441–452.

Schauf, C. L., and M. A. Chuman. 1986. Mechanisms of sodium channel gating revealed by solvent substitution. *In* Neural Membranes. Alan R. Liss, Inc., New York. 3–23.

Shrager, P. 1974. Ionic conductance changes in voltage clamped crayfish axons at low pH. *J. Gen. Physiol.* 64:666–690.

Starkus, J. G., and P. Shrager. 1978. Modification of slow sodium inactivation in nerve after internal perfusion with trypsin. *Am. J. Physiol.* 4:C238–244.

Stimers, J. R., F. Bezanilla, and R. E. Taylor. 1985. Sodium channel activation in the squid giant axon. Steady state properties. *J. Gen. Physiol.* 85:65–82.

Stimers, J. R., F. Bezanilla, and R. E. Taylor. 1987. Sodium channel gating currents. Origin of the rising phase. *J. Gen. Physiol.* 89:521–540.

Stühmer, W., F. Conti, H. Suzuki, X. Wang, M. Noda, N. Yahagi, H. Kubo, and S. Numa. 1989. Structural parts involved in activation and inactivation of the sodium channel. *Nature (Lond.).* 339:597–603.

Swain, C. G., and D. F. Evans. 1966. Conductances of ions in light and heavy water at 25°C. *J. Am. Chem. Soc.* 88:383–390.

Taylor, R. E., and F. Bezanilla. 1983. Sodium and gating current time shifts resulting from changes in initial conditions. *J. Gen. Physiol.* 81:773–784.

Wang, G. K., M. S. Brodwick, and D. C. Eaton. 1985. Removal of sodium channel inactivation in squid axon by the oxidant chloramine-T. *J. Gen. Physiol.* 86:289–302.

Woodbury, J. W. 1971. Eyring rate theory model of the current-voltage relationships of ion channels in excitable membranes. *In* Chemical Dynamics: Papers in Honor of Henry Eyring. J. O. Hirschfelder, editor. John Wiley & Sons, New York. 601–617.